International Journal of Thermophysics, Vol. 14, No. 1, 1993

Thermal Conductivity of Halogenated Ethanes, HFC-134a, HCFC-123, and HCFC-141b

R. Yamamoto,[1] S. Matsuo,[2] and Y. Tanaka[2]

Received August 31, 1992

The gaseous thermal conductivity of three CFC alternatives, HFC-134a (1,1,1,2-tetrafluoroethane), HCFC-123 (1,1-dichloro-2,2,2-trifluoroethane), and HCFC-141b (1,1-dichloro-1-fluoroethane), has been measured in the temperature ranges 273–363 K (HFC-134a) and 313–373 K (HCFC-123, HCFC-141b) at pressures up to saturation. The measurements were performed with a new improved transient hot-wire apparatus. The uncertainty of the experimental data is estimated to be within 1%. The gaseous thermal conductivity obtained in this work together with the liquid thermal-conductivity data from the literature were correlated with temperature and density by an empirical equation based on the excess thermal-conductivity concept. The equation is found to represent the experimental results with average deviations of 2.5% for HFC-134a, 0.75% for HCFC-123, and 0.55% for HCFC-141b, respectively.

KEY WORD: halogenated ethane; HCFC-123; HCFC-141b; HFC-134a; thermal conductivity; transient hot-wire method.

1. INTRODUCTION

As is well-known, halogenated ethanes HFC-134a, HCFC-123, and HCFC-141b are expected to be promising CFC alternative refrigerants. Accurate knowledge of thermophysical properties are required to use these fluids in various energy systems and for other applications. Concerning the thermal conductivity, the transient hot-wire method is now widely accepted as the most accurate and reliable method for the measurement of the thermal conductivity of fluids. Several measurements by the transient hot-wire method have been reported for these halogenated ethanes [2–10]. However, accurate measurements of the thermal conductivity of dilute

[1] Division of Molecular Engineering, Kyoto University, Kyoto 606-01, Japan.
[2] Department of Applied Chemistry, Kobe University, Kobe 657, Japan.

0195-928X/93/0100-0079$07.00/0

gases are quite difficult, because the diameter of platinum wire is required to be very thin (less than 10 μm for halogenated ethanes). In this work, the transient hot-wire apparatus was improved by the use of a 5-μm-diameter platinum wire and recent computerized measuring instruments.

It is also important to improve the correlating equations to represent the thermal conductivity over wide temperature and pressure ranges. We also present useful correlations for these fluids on the basis of the excess thermal-conductivity concept.

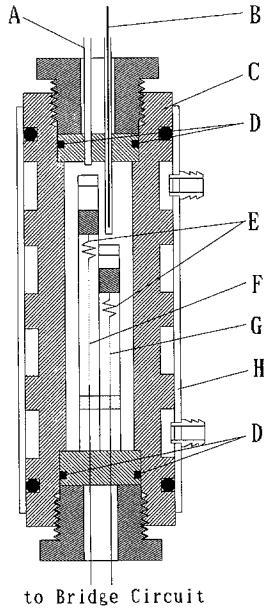

Fig. 1. The thermal-conductivity measuring cell. (A) Sample inlet. (B) Thermistor. (C) High-pressure vessel (brass, o.d. = 70 mm, i.d. = 35 mm, $l = 200$ mm). (D) O-ring. (E) Copper spring. (F) Main Pt wire ($d = 5$ μm, $l = 50$ mm). (G) Compensating Pt wire ($d = 5$ μm, $l = 25$ mm). (H) Water jacket (stainless steel).

2. EXPERIMENTAL

The measurements were performed with a new improved transient hot-wire apparatus. The working equation is given by [1]

$$\Delta T = \frac{q}{4\pi\lambda} \ln \frac{4\kappa t}{a^2 C} \tag{1}$$

where ΔT is the temperature rise of the platinum wire, q is the power input per unit length of the platinum wire, λ is the thermal conductivity and κ is the thermal diffusivity of the sample fluid, a is the radius of the platinum wire, and C is the exponential of Euler's constant.

Accurate measurements of the thermal conductivity of dilute gases are difficult because the diameter of platinum wire must be sufficiently thin (less than 10 μm for halogenated ethanes). In this work, we use a 5-μm-diameter platinum wire to minimize the influence of the heat capacity of the wire on the measurements. A cross-sectional view of the cell is shown in Fig. 1.

Figure 2 shows the bridge circuit to measure the temperature rise of the platinum wire. The main Pt wire and the compensating wire are arranged in opposing arms of a bridge circuit to cancel the edge effect of the hot wire [2]. As R1 and R2 increase following initiation of the heating cycle, the bridge deviates from the balance point. The out-of-balance voltage is amplified and measured at a frequency of 30 kHz using analog–digital transfer. In this apparatus, the PC control the measurement cycle and calculate the thermal conductivity automatically. The maximum uncertainty in the experimental data is estimated to be within 1%.

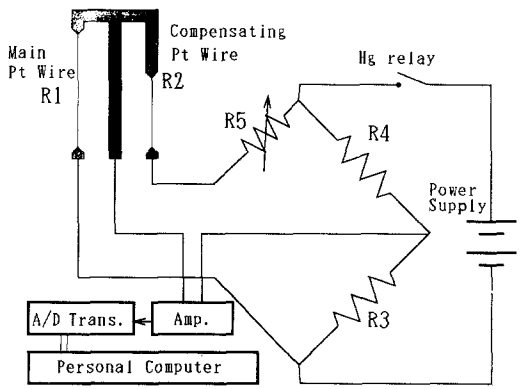

Fig. 2. The bridge circuit.

Table I. Thermal Conductivity of Gaseous HFC-134a

Temperature (K)	Pressure (MPa)	Density ($kg \cdot m^{-3}$)	Thermal conductivity ($mW \cdot m^{-1} \cdot K^{-1}$)
273.15	0.10	4.62	10.96
283.15	0.10	4.44	11.83
	0.20	9.11	11.89
	0.30	14.06	11.95
	0.40	19.35	12.03
303.15	0.10	4.12	13.43
	0.20	8.41	13.46
	0.30	12.88	13.43
	0.40	17.57	13.58
	0.57	25.85	13.69
	0.72	34.13	13.88
323.15	0.10	3.85	15.03
	0.30	11.93	15.15
	0.50	20.59	15.20
	0.70	29.95	15.18
	0.90	40.22	15.36
	1.10	51.68	15.57
	1.26	62.24	15.75
343.15	0.10	3.62	16.44
	0.20	7.33	16.55
	0.30	11.13	16.55
	0.40	15.04	16.54
	0.50	19.06	16.60
	0.60	23.20	16.62
	0.80	31.87	16.80
	1.00	41.17	16.81
	1.20	51.21	16.88
	1.40	62.18	17.16
	1.60	74.37	17.32
	1.80	88.19	17.75
	2.01	105.30	18.28
363.15	0.56	19.87	18.12
	1.02	38.51	18.35
	1.50	60.55	18.82
	2.00	87.93	19.10
	2.41	115.21	19.98
	2.80	150.08	20.36
	3.05	180.66	21.86

Table II. Thermal Conductivity of Gaseous HCFC-123

Temperature (K)	Pressure (MPa)	Density ($kg \cdot m^{-3}$)	Thermal conductivity ($mW \cdot m^{-1} \cdot K^{-1}$)
313.15	0..10	6.19	10.98
	0.13	8.30	11.01
333.15	0.10	5.77	11.96
	0.20	11.78	12.09
353.15	0.10	5.41	12.81
	0.20	10.96	12.98
	0.29	16.25	13.22
	0.44	25.86	13.28
373.15	0.10	5.10	13.90
	0.25	13.04	13.92
	0.41	22.36	14.30
	0.55	30.45	14.46
	0.72	41.98	14.72

The sample fluids, HFC-134a, HCFC-123, and HCFC-141b, were synthesized and purified by Daikin Industries, Ltd., with purities better than 99.9%. These fluids were used without further purification.

3. RESULTS

The experimental results for gaseous HFC-134a, HCFC-123, and HCFC-141b are listed in Tables I to III. The densities were obtained from

Table III. Thermal Conductivity of Gaseous HCFC-141b

Temperature (K)	Pressure (MPa)	Density ($kg \cdot m^{-3}$)	Thermal conductivity ($mW \cdot m^{-1} \cdot K^{-1}$)
313.15	0.10	4.69	11.27
	0.12	5.68	11.29
333.15	0.10	4.39	12.08
	0.15	6.58	12.24
	0.21	9.22	12.24
353.15	0.10	4.12	13.12
	0.20	8.49	13.16
	0.34	14.62	13.47
373.15	0.10	3.89	14.33
	0.29	11.58	14.64
	0.37	14.88	14.93
	0.48	19.98	14.95
	0.60	25.45	15.14

Table IV. Coefficients in Eq. (2)

	HFC-134a	HCFC-123	HCFC-141b
a_1	1.21874×10^{-2}	2.41609×10^{-2}	2.37350×10^{-2}
a_2	1.04545×10^{-4}	3.48548×10^{-5}	3.88592×10^{-5}

the equations of states determined by Piao et al. for HFC-134a [11] and by the Japanese Association of Refrigeration and the Japan Flon Gas Association (JAR-JFGA) for HCFC-123 [4]. The densities of HCFC-141b were calculated from the SRK equation of states using the critical parameters, $T_c = 481.3$ K, $P_c = 4.256$ MPa, and acentric factor of 0.207.

3.1. Thermal Conductivity at Atmospheric Pressure

The gaseous thermal conductivity of these fluids at atmospheric pressure λ^{atm} is correlated by a polynomial of temperature.

$$\lambda^{atm}(T) = a_1 T + a_2 T^2 \tag{2}$$

with λ^{atm} in $mW \cdot m^{-1} \cdot K^{-1}$ and T in K. The coefficients in Eq. (2) for each fluid are listed in Table IV. The validity of this equation is 270–380 K for HFC-134a and 300–380 K for HCFC-123 and HCFC-141b.

3.2. Thermal Conductivity of Saturated Vapor

The saturated vapor thermal conductivity λ^{sat} was determined by the extrapolation of experimental data along the isotherms to saturation pressures. The λ^{sat} values obtained are correlated by the following equation as a function of temperature:

$$\lambda^{sat}(T) = b_1 T + b_2 T^2 + b_3 \frac{T}{T_c - T} \tag{3}$$

Table V. Coefficients in Eq. (3)

	HFC-134a	HCFC-123	HCFC-141b
b_1	-5.0315×10^{-3}	1.8005×10^{-2}	2.68954×10^{-3}
b_2	1.6361×10^{-4}	4.8410×10^{-5}	0
b_3	9.7271×10^{-2}	2.9985×10^{-1}	1.5092
T_c	374.30	456.86	481.3

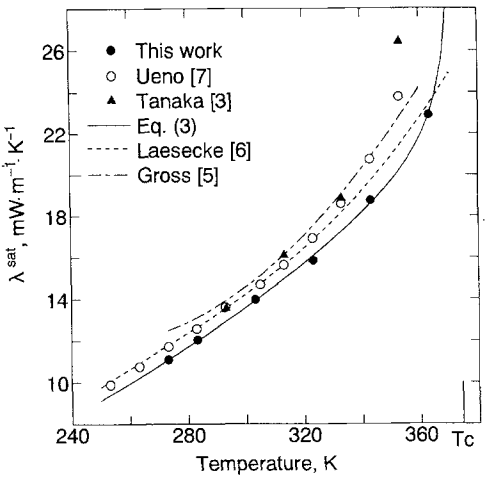

Fig. 3. Thermal conductivity of gaseous HFC-134a at saturation.

with λ^{sat} in $mW \cdot m^{-1} \cdot K^{-1}$ and T in K. The coefficients in Eq. (3) for each fluid are listed in Table V. The validity of this equation is 270–370 K for HFC-134a and 300–380 K for HCFC-123 and HCFC-141b. In Figs. 3–5, the saturated vapor thermal conductivity for each fluid is plotted together with some literature values as a function of temperature. Good agreements

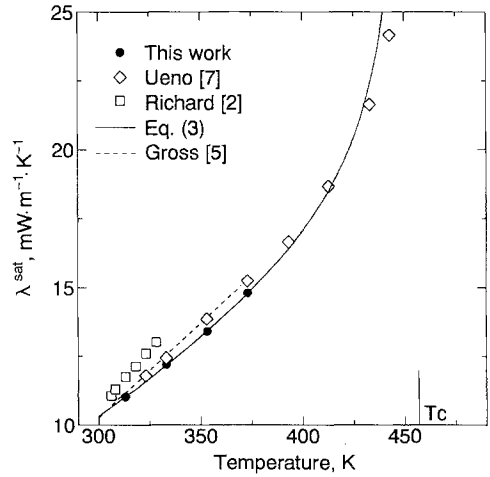

Fig. 4. Thermal conductivity of gaseous HCFC-123 at saturation.

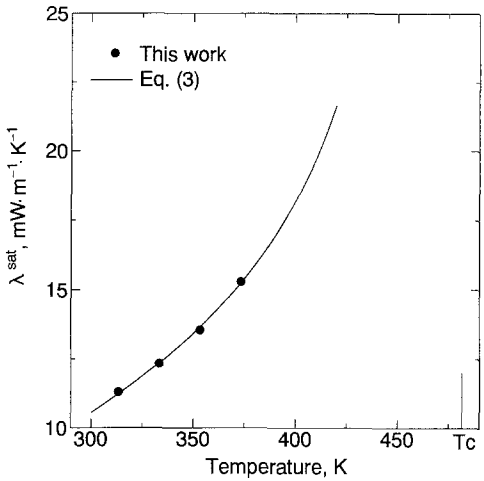

Fig. 5. Thermal conductivity of gaseous HCFC-141b at saturation.

are observed within mutual experimental uncertainties for HFC-134a and HCFC-123. There are few reports on the gaseous thermal conductivity of HCFC-141b.

4. CORRELATION

To correlate the thermal conductivity in a wide range of temperature and pressure, it is convenient to divide the thermal conductivity into three contributions, namely, the zero-density thermal conductivity $\lambda^0(T)$, the density-dependent excess thermal conductivity $\lambda^{ex}(\rho)$, and the critical enhancement $\lambda^{cr}(T, \rho)$. Since few measurements were performed in the critical region for these CFC alternatives, the critical enhancement λ^{cr} is omitted in this work.

$$\lambda(T, \rho) = \lambda^0(T) + \lambda^{ex}(\rho) \tag{4}$$

Figures 6–8 show deviation plot of data used in this correlation relative to our correlation.

4.1. Zero-Density Thermal Conductivity

The zero-density thermal conductivity λ^0 of these fluids was determined by the extrapolation of experimental data along the isotherms to

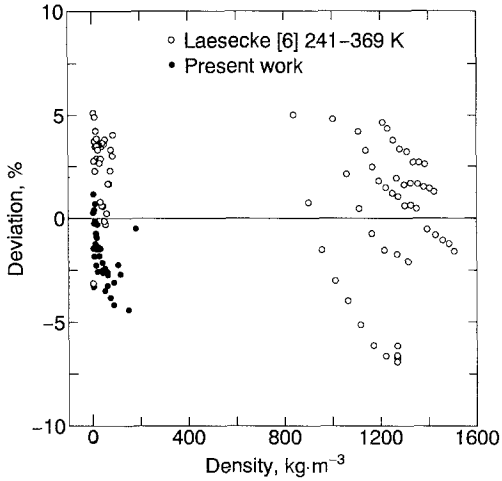

Fig. 6. Deviation plot of experimental data used in this correlation relative to Eq. (4) for HFC-134a.

zero density. The zero-density thermal conductivity is correlated by the following equation as a function of temperature:

$$\lambda^0(T) = c_1 T + c_2 T^2 \tag{5}$$

with λ^0 in $\mathrm{mW \cdot m^{-1} \cdot K^{-1}}$ and T in K. The coefficients in Eq. (5) for each fluid are listed in Table VI. The validity of this equation is 270–380 K for HFC-134a and 300–380 K for HCFC-123 and HCFC-141b.

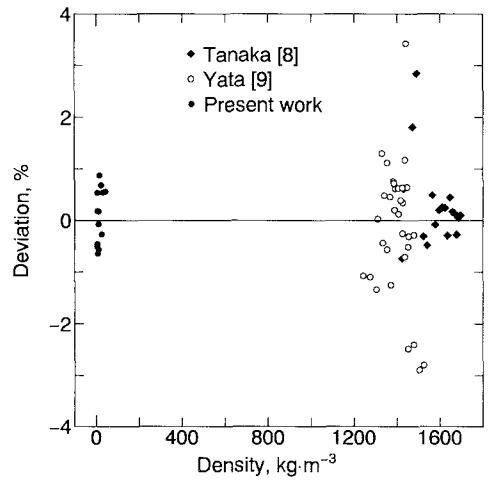

Fig. 7. Deviation plot of experimental data used in this correlation relative to Eq. (4) for HCFC-123.

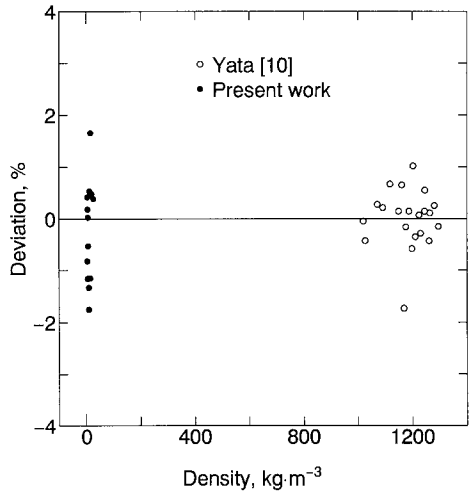

Fig. 8. Deviation plot of experimental data used in this correlation relative to Eq. (4) for HCFC-141b.

4.2. Excess Thermal Conductivity

The excess thermal conductivity λ^{ex} was deduced from our gaseous data together with liquid data cited from literature. It is difficult to separate the excess thermal conductivity and the thermal conductivity critical enhancement. Fortunately, no significant critical enhancement was observed in experimental data used in this correlation for HCFC-123 and HCFC141b. For HFC-134a, experimental data clearly contain critical enhancement near the critical temperature. Thus we did not use Laesecke's data of 393 K to determine λ^{ex} for HFC-134a. λ^{ex} is correlated by

$$\lambda^{ex}(\rho) = d_1\rho + d_2\rho^2 + d_3\rho^3 + d_4\rho^4 \tag{6}$$

with λ^{ex} in $mW \cdot m^{-1} \cdot K^{-1}$ and ρ in $kg \cdot m^{-3}$. The coefficients in Eq. (6) for each fluid are listed in Table VII. The validity of this equaion is

Table VI. Coefficients in Eq. (5)

	HFC-134a	HCFC-123	HCFC-141b
c_1	1.5974×10^{-2}	2.4672×10^{-2}	2.2343×10^{-2}
c_2	9.1981×10^{-5}	3.2378×10^{-5}	4.1542×10^{-5}

Table VII. Coefficients in Eq. (6)

	HFC-134a	HCFC-123	HCFC-141b
d_1	2.3334×10^{-2}	2.1608×10^{-2}	3.8267×10^{-2}
d_2	-8.5451×10^{-6}	1.0135×10^{-5}	-2.1368×10^{-5}
d_3	1.5221×10^{-8}	-3.0192×10^{-8}	-1.1777×10^{-8}
d_4	1.1350×10^{-11}	2.3559×10^{-11}	3.7871×10^{-11}

$\rho < 1500\ \mathrm{kg \cdot m^{-3}}$ for HFC-134a, $\rho < 1700\ \mathrm{kg \cdot m^{-3}}$ for HCFC-123, and $\rho < 1300\ \mathrm{kg \cdot m^{-3}}$ for HCFC-141b. The data sources used in this correlation are summarized in Table VIII.

5. CONCLUSION

The gaseous thermal conductivity of three halogenated ethanes, HFC-134a, HCFC-123, and HCFC-141b, has been measured with a new improved transient hot-wire apparatus with an estimated uncertainty of 1%. The thermal conductivities at atmospheric and saturated pressures are

Table VIII. Data Source Used in this Correlation

Ethane	Property	Source(s)
HFC-134a	λ	
	Gas	This work and Laesecke et al. [6]
	Liquid	Laesecke et al. [6]
	ρ	
	Gas and liquid	Piao et al. [11]
HCFC-123	λ	
	Gas	This work
	Liquid	Tanaka et al. [8] and Yata et al. [9]
	ρ	
	Gas and liquid	JAR-JFGA [4]
HCFC-141b	λ	
	Gas	This work
	Liquid	Yata [10]
	ρ	
	Gas	SRK eq. (estimation)
	Liquid	Yoshimoto [12]

correlated as functions of temperature. Comparisons of the data obtained with previous data from the literature show good agreement within mutual experimental uncertainty for HFC-134a and HCFC-123. Concerning HCFC-141b, there are few reports on the gaseous thermal conductivity; thus, this paper provides valuable data.

The gaseous thermal conductivity obtained in this study and the liquid thermal conductivity cited from the literature were correlated with temperature and density by an empirical equation based on the excess thermal-conductivity concept. This equation is found to represent the experimental results with average deviations of 2.5% for HFC-134a, 0.75% for HCFC-123, and 0.55% for HCFC-141b, respectively.

ACKNOWLEDGMENTS

The authors are indebted to Daikin Industries, Ltd., for furnishing the sample fluids. The financial support for this work was provided in part by a Grant-in-Aid for Scientific Research from the Ministry of Education, Japan.

REFERENCES

1. J. J. de Groot, J. Kestin, and H. Sookiazian, *Physica* **75**:454 (1974).
2. R. G. Richard and I. R. Shankland, *Int. J. Thermophys.* **10**:673 (1989).
3. Y. Tanaka, M. Nakata, and T. Makita, *Int. J. Thermophys.* **12**:949 (1991).
4. JAR-JFGA, *Thermophysical Properties of Environmentally Acceptable Fluorocarbons, HFC-134a and HCFC-123* (JAR, Tokyo, 1991).
5. U. Gross, Y. W. Song, J. Kallweit, and E. Hahne, *Proc. I.I.F.-I.I.R.-Commission B1*, Tel Aviv (1990).
6. A. Laesecke, R. A. Perkins, and C. A. Nieto de Castro, *Fluid Phase Equil.* (in press).
7. Y. Ueno, Y. Nagasaka, and A. Nagashima, *Proc. 12th Jpn. Symp. Thermophys. Prop.*, Kyoto (1991), p. 225.
8. Y. Tanaka, A. Miyake, H. Kashiwagi, and T. Makita, *Int. J. Thermophys.* **9**:465 (1988).
9. J. Yata, C. Kawashima, M. Hori, and T. Mimamiyama, in *Proc. 2nd Asian Thermophys. Prop. Conf.*, Sapporo, N. Seki and B. X. Wang, eds. (1989), p. 201.
10. J. Yata, Personal communication (1991).
11. C.-C. Piao, H. Sato, and K. Watanabe, in press.
12. T. Yoshimoto, M.S. thesis (Kobe University, Kobe, 1990).